Polymer Chemistry

This article can be cited before page numbers have been issued, to do this please use: P. Xu, I. Murtaza, J. Shi, M. Zhu, Y. He, H. Yu, O. Goto and H. Meng, *Polym. Chem.*, 2016, DOI: 10.1039/C6PY00989A.

ROYAL SOCIETY OF CHEMISTRY

www.rsc.org/polymers

View Article Online
DOI: 10.1039/C6PY00989A

Journal Name

ARTICLE

Highly Transmissive Blue Electrochromic Polymers Based On Thieno[3,2-*b*]thiophene

Received 00th January 20xx,
Accepted 00th January 20xx

DOI: 10.1039/x0xx00000x

www.rsc.org/

Panpan Xu,[a] Imran Murtaza,[b,c] Jingjing Shi,[a] Mengmeng Zhu,[a] Yaowu He,[a] Hongtao Yu,[b] Osamu Goto,[a] Hong Meng*[,a]

A series of three polymers based on thieno[3,2-*b*]thiophene core are synthesized and polymerized via electrochemical polymerization. The addition of benzene and thiophene rings as two different type of substituents on the 3,6-position of thieno[3,2-*b*]thiophene core bring about variance in color changing, optical contrast and morphological demeanor. Electrochromical studies demonstrate that **P1** and **P2** switch between deep blue neutral and colorless transparent oxidized states, while **P3** switches between violet and light green transmissive states. Amid the three polymers, **P1** shows the highest optical contrast (71%) in the visible region with a complete coloring and bleaching in just 1.10 s and 1.80 s, respectively, in addition, all three polymers reveal about 60% of the transmittance change in near-IR region, which render them commendable application in NIR electrochromic devices. AFM images depict an augmented surface roughness due to the introduction of alkyl chains in the thieno[3,2-*b*]thiophene core, which give rise to better stability of the polymer thin film.

Introduction

The 2000 Nobel Prize in chemistry manifested the momentous role of conducting macromolecules in academia. As an embranchment of conducting macromolecules, electrochromic polymers have triggered extensive research in recent years. Electrochromism may be defined as the acclimatization of optical properties through redox processes.[1] Compared with inorganic materials, conducting polymers enjoy the great advantages, such as higher coloration efficiency, higher optical contrast, lower oxidation potential, faster switching time, easier fine-tuning of the band gap with modification of chemical structures and possibility of large-area device fabrication. Based on their advantages, conducting polymers have extensive applications encompassing smart windows,[2] displays,[3] sunglasses, anti-glare rear-view mirrors,[4] and resistance random access memory (RRAM) due to a memory effect of conducting polymers.[5]

Notwithstanding the discovery of green[6-8] or yellow[9] to transmissive electrochromic polymer materials resolved the problems of additive and subtractive color space in electrochromic field, the search for polymers with better stable color-switching, higher optical contrast and faster switching time still persists. Blue component plays an indispensible role in achieving RGB (red, green, blue)-based electrochromic device applications, in addition, colorless transparency at oxidized state is also vital because the optical contrast ratio between the two states decides the electrochromic application of the materials. Compared with the polymers which transform from green to transmissive state, requiring two absorption bands in UV-Vis region, the electrochromic polymers which switch from blue to transmissive state just need a single absorption band in the visible region, which provides a simple structural design idea. PEDOT, a classic electrochromic polymer with low oxidation potential and moderate band gap has the ability to transform from deep blue neutral state to a sky-blue transmissive oxidized state.[10] Later, many attempts have been made to embellish PEDOT structure to obtain blue-to-highly transmissive switching polymers, such as replacing the S atom with the Se atom,[11, 12] varying the size and composition of the alkylene bridge[13] and introducing hydrophilic groups.[14] Moreover, the employing of donor-acceptor type structure flexible to modulate the absorption of the objective donor-acceptor polymers[15] also gives rise to electrochromic polymers switching from blue to colorless transmissive state.[16, 17]

Thieno[3,2-*b*]thiophene unit possesses rigid structure with an extended π-conjugation, which is beneficial to adjust the band gap and increase intermolecular interactions in the solid state organic materials,[18] initiating its extensive use in organic

---

[a] *School of Advanced Materials, Peking University Shenzhen Graduate School, Shenzhen, 518055, China.*

[b] *Key Laboratory of Flexible Electronics (KLOFE) & Institute of Advanced Materials (IAM), Jiangsu National Synergetic Innovation Center for Advanced Materials (SICAM), Nanjing Tech University (Nanjing Tech), 30 South Puzhu Road, Nanjing 211816, China.*

[c] *Department of Physics, International Islamic University, Islamabad 44000, Pakistan*

† *Tel: (86)-18565807998, E-mail: menghong@pkusz.edu.cn*

Electronic Supplementary Information (ESI) available: synthetic routes and characterization for all the intermediates; SEM topography images and cyclic voltammetry stability test of polymer-coated ITO films; movies for reversible switching colours of polymer based devices between neutral and oxidized states. ^{1}H and ^{13}C NMR spectra for target monomers; See DOI: 10.1039/x0xx00000x

View Article Online
DOI: 10.1039/C6PY00989A

photovoltaics (OPV)[19] and thin-film transistors (OTFTs).[20] However, electrochromism in thieno[3,2-*b*]thiophene incorporated PEDOT needs to be explored further.

In this study, we combined thieno[3,2-*b*]thiophene conjugated unit with PEDOT and envisioned that the corresponding polymers have a lower band gap which is favorable to cathodically coloring polymers with highly transmissive oxidized states.[21] In order to further improve the processibility, we introduced different substituents into 3,6-position of thieno[3,2-*b*]thiophene core. Based on the previous studies demonstrating that substituents in conjugated backbone bring about great influence on electrochromic properties,[22, 23] such as the employment of bulky *t*-butyl substituents shows a meaningful strength in redox stability, electron donating alkoxy groups function in modulating the oxidation potentials and bandgap of the corresponding polymers,[24] in addition, steric replusion induced by substituents also affects the conformation of the conjugated backbone,[23] then we anticipate that the long alkyl chain substitution effect and addition of benzene or thiophene rings can give rise to the splendid electrochromic properties, so we synthesized monomers **M1**, **M2** and **M3** (Scheme 1). The state and color of the three monomers appeared solid and yellow. All the monomers presented good solubility, which made the electrochemical polymerization possible to prepare the corresponding polymers (**P1**, **P2** and **P3**). Hitherto there are few systematic studies regarding the substituents influences on electrochromic behaviors, herein we compare the influence of different types of substituents on spectra for color control according to their electrochemical and spectroelectrochemical properties characterized by cyclic voltammetry, UV-Vis-NIR spectroscopy, AFM (Atom Force Microscopy) and SEM (Scanning Electron Microscopy). **P1** and **P2** exhibit a color change from deep blue to transparent colorless state while **P3** switches between violet and transmissive light green color. The high optical contrast of **P1** (71%) makes it an attractive candidate in absorption/transmissive device applications, such as optical shutters, e-paper and so on. The stability of **P2** exerts a great improvement (an increase of about 27%) owing to the adopting of alkyl chain compared to **P1**. All the above properties give a commendable understanding of color-tuning via structure control.

Experimental

Chemicals and Instrumentation

All chemicals were purchased from Aldrich, dichloromethane (DCM) was dried and distilled over calcium hydride under nitrogen atmosphere, acetonitrile (ACN) was purified and dried by organic solvent purification system from Vacuum Atmospheres. The electrochemical measurements were performed using a CHI620E electrochemical workstation and UV–Vis–NIR spectra was studied using a Lambda 750 spectrophotometer. The structure of compounds was detected by NMR (Bruker, AVANCE 300 MHz) and HRMS (Thermo, Q-Exactive). The thickness of polymer films coated on ITO glass slides was measured by the Bruker DEKTAK XT Profilometer.

Representative procedure for the synthesis of monomers

Compound **3** (5 mmol) and tributyl(2,3-dihydrothieno[3,4-*b*][1,4]dioxin-5-yl)stannane (compound **4**, 25 mmol) were dissolved in dry THF (500 mL). The solution was purged with nitrogen for 30 min, then Pd(PPh$_3$)$_2$Cl$_2$ (1.35 mmol, 27%) was added at room temperature under nitrogen atmosphere. The mixture was stirred at 90 °C under nitrogen atmosphere for 15 h. Then cooled and concentrated on the rotary evaporator. The residue was subjected to column chromatography (CH$_2$Cl$_2$:petroleum = 3:1) to get the yellow solid. The synthetic route of the three monomers are shown in Scheme 1.

5,5'-(3,6-bis(4-hexylphenyl)thieno[3,2-*b*]thiophene-2,5-diyl)bis(2,3-dihydrothieno[3,4-*b*][1,4]dioxine) (**M1**). 60% yield. ^{1}H NMR (300 MHz, CDCl$_3$, ppm): δ 7.54 (d, *J* = 9.0 Hz, 4H), 7.42 (d, *J* = 9.0 Hz, 6H), 6.24 (s, 2H), 4.12 (s, 4H), 4.07 (s, 4H). ^{13}C NMR (300 MHz, CDCl$_3$, ppm): δ 141.40, 139.22, 138.87, 135.36, 131.80, 129.65, 129.26, 128.79, 128.07, 111.18, 99.94, 64.83, 64.56. HRMS (+ESI), *m/z* calcd. for $C_{30}H_{20}O_4S_4$ $(M+H)^+$ 573.0323, found 573.0315.

5,5'-(3,6-diphenylthieno[3,2-b]thiophene-2,5-diyl)bis(2,3-dihydrothieno[3,4-*b*][1,4]dioxine) (**M2**): 65% yield. ^{1}H NMR (300 MHz, CDCl$_3$, ppm): δ 7.43 (d, *J* = 9.0 Hz, 4H), 7.22 (d, *J* = 9.0 Hz, 4H), 6.23 (s, 2H), 4.14-4.11 (m, 4H), 4.07-4.05 (m, 4H), 2.65 (t,4H), 1.71-1.61 (m, 4H), 1.40-1.27 (m, 12H), 0.90 (t,6H). ^{13}C NMR (300 MHz, CDCl$_3$, ppm): δ 142.88, 141.35, 139.20, 138.75, 132.51, 131.92, 129.19, 129.03, 128.77, 111.46, 99.76, 64.80, 64.55, 35.99, 31.88, 31.50, 29.16, 22.78, 14.26. HRMS (+ESI), *m/z* calcd. for $C_{42}H_{44}O_4S_4$ $(M+H)^+$ 741.2201, found 741.2195.

5,5'-(3,6-bis(5-hexylthiophen-2-yl)thieno[3,2-*b*]thiophene-2,5-diyl)bis(2,3-dihydrothieno[3,4-b][1,4]dioxine) (**M3**): 68% yield. ^{1}H NMR (300 MHz, CDCl$_3$, ppm): δ 7.11 (d, *J* = 3.0 Hz, 2H), 6.74 (d, *J* = 3.0 Hz, 2H), 6.41 (s, 2H), 4.19 (s, 8H) 2.80 (t, 4H), 1.72-1.62 (t, 4H), 1.42-1.25 (t, 12H), 0.89 (t, 6H). ^{13}C NMR (300 MHz, CDCl3, ppm): δ 147.02, 141.49, 140.16, 138.30, 133.24, 128.60, 126.87, 126.41, 124.13, 109.99, 101.04, 64.94, 64.65, 31.74, 31.71, 30.30, 28.92, 22.74, 14.24. HRMS (+ESI), *m/z* calcd. for $C_{38}H_{40}O_4S_6$ $(M+H)^+$ 753.1329, found 753.1323.

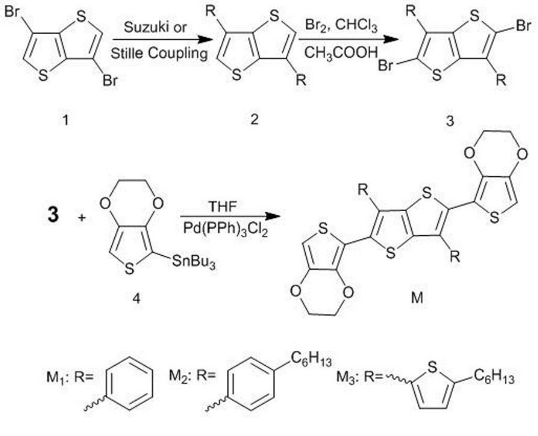

Scheme 1 Synthetic routes of monomers **M1**, **M2** and **M3**

View Article Online
DOI: 10.1039/C6PY00989A

Results and discussion

Electropolymerization and Electrochemical properties

Electrochemical measurements were performed in a three-electrode cell with a polymer-coated Pt button electrode (area: 0.0314 cm^2) as the working electrode, a Pt wire as the counter electrode and a Ag wire as the reference electrode containing 0.001 M monomer with 0.1 M DCM/ACN/TBAPF$_6$ (tetrabutylammonium hexafluorophosphate) as solvent-electrolyte couple. The potentials were scanned between -0.8 V and 1.4 V at a scan rate of 100 mV s^{-1} for 8 cycles for **M2**, **M3** (while between -0.4 V and 1.4 V at a scan rate of 100 mV s^{-1} for 5 cycles and only DCM as single solvent for **M1** because of the easy film-processing ability) as shown in Fig. 1(a), (b) and (c). In the first cycle, the oxidation of the monomers stars at 0.69 V for **M1**, 0.72 V for **M2** and 0.83 V for **M3** *versus* Ag wire pseudo-reference electrode. After a number of cycles, electroactive thin films were deposited on the working electrode surface which appeared purple in color. The different intermolecular interactions brought by substituents lead to a thinner and flat surface of **P1** film while the thicker **P2** and **P3** films with mini granular surface, the films thickness are 59 nm for **P1**, 97 nm for **P2** and 107 nm for **P3,** respectively. The corresponding results of cyclic voltammetry measurements are summarized in Table 1. As seen from Fig. 1d, combined with backbone planarity and conjugation, the insulating character of aliphatic chain attached to benzene or thiophene ring and the electro-rich property of substituents[25], the onsets of oxidation are located at 0.07 V, 0.10 V and 0.15 V for **P1**, **P2** and **P3** respectively *vs*. the same reference electrode. Maybe the lowest onset of oxidation about **P1** indicates the planar, electro-rich nature of phenyl in 3,6-position of thieno[3,2-*b*]thiophene core, which can more effectively stabilize the positive charge carriers formed during oxidation[13]. On the basic of redox potentials of ferrocene/ferrocenium reference (F_c/F_c^+ *versus* Ag wire pseudo-reference electrode, 0.52 V) and the onset of oxidation peaks, the HOMO levels are estimated to be –4.35 eV for **P1**, -4.38 eV for **P2** and -4.43 eV for **P3**, respectively. The bandgap of **P1**, **P2**, **P3** are 1.80 eV, 1.78 eV and 1.70 eV as determined from the λ_{edge} of three polymers, 688 nm, 698 nm and 731 nm (Fig. 2), respectively. The corresponding LOMO levels are calculated to be -2.55 eV, -2.60 eV and -2.73 eV for **P1**, **P2** and **P3**, respectively. Comparing with **P1** and **P2**, **P3** shows the highest $E_{1/2}$ due to the lower conductivity, which is mainly because of the the electrical insulating property of alkyl chain.[26]

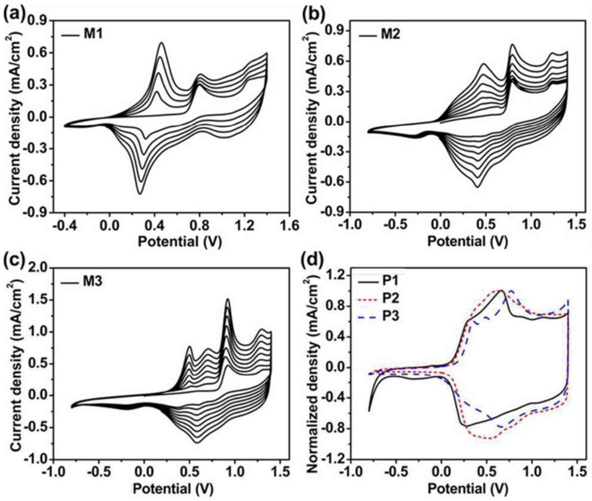

Fig. 1 Repeated scan electropolymerization on a Pt button electrode at a scan rate of 100 mV s^{-1} in (a) (b) 0.1 M TBAPF$_6$/DCM/ACN (V:V = 3:1) for **M1**, **M2** (c) 0.1 M TBAPF$_6$/DCM for **M3** (d) Single scan cyclic voltammetry of three polymers on polymer-coated Pt electrode in 0.1 M TBAPF$_6$/ACN at a scan rate of 100 mV s^{-1}.

Table 1 Electrochemical and optical properties of polymers

Polymers	E_{ox} onset (V)	$E_{p,ox}$ (V)	$E_{p,red}$ (V)	E_{HOMO} (eV)^a	E_{LUMO} (eV)^b	$E_{g,opt}$ (eV)^c
P1	0.07	0.66	0.28	-4.35	-2.55	1.80
P2	0.10	0.63	0.53	-4.38	-2.60	1.78
P3	0.15	0.77	0.66	-4.43	-2.73	1.70

$^a E_{HOMO}$= -($E_{[onset, ox\ vs.\ Fc/Fc+]}$ + 4.8) (eV)[27]. $^b E_{LUMO}$=(E_{HOMO} +$E_{g,opt}$). ^{c}Obtained from the absorption edge as seen in Fig. 2 at the voltage of 0 V

Spectroelectrochemistry

To compare the optical property at different applied potentials, the in situ spectroelectrochemical measurements were performed using UV-Vis-NIR spectrophotometer in combination with potentiostat/galvanostatic in 0.l M TBAPF$_6$/ACN system. Polymer films were deposited on ITO glass slides through electropolymerization method. As shown in Fig. 2(a) and (b), at lower potentials, **P1** and **P2** show the same splitted absorption peaks located at 585 nm and 640 nm for **P1**, 595 nm and 650 nm for **P2**, which can be ascribed to the formation of a well-organized and more rigid polymer backbone[11, 12] and also explains the similarity in color changing

View Article Online
DOI: 10.1039/C6PY00989A

effect of the two polymers at neutral state. *L*a*b** defines the color/light transmission changes of elecrochromic polymers in terms of the external applied bias.[28] **P1** and **P2** are deep blue in neutral state, the *L*a*b** values are (30.5, 3.9, -8.9) and (25.7, 2.8, -11.7) respectively. For **P1**, the two splitted peaks reach a maximum intensity at -0.3 V, the intensity of absorption peaks at 585 nm and 640 nm decreases with the increase of applied potential from -0.3 V to 1.2V. **P2** shows the similar changing tendency. When the polymers are gradually oxidized at higher potentials, the absorption peaks in the visible region of three polymers deplete while the strong and broad absorption bands (at about 900nm) appear in near-IR region because of the formation of polarons. When further oxidized, the extended absorptions at about 1400 nm increase because the polarons are converted to bipolarons,[29] at the same time, the color of the films of **P1** and **P2** changes from deep blue to transparent colorless state, the corresponding *L*a*b** values are (33.9, -4.0, -13.5) and (35.0, -5.1, -15.5) respectively. **P3** has a broad absorption in visible region (located at about 540 nm), which results in a violet color in neutral state, the emergence of a tailing in the near-IR (800-1000 nm) in its oxidized state (1.4 V) generates a light green transmissive oxidized state of **P3** while **P1** and **P2** are highly colorless transimissive.[13] The *L*a*b** values of **P3** are (24.8, 1.9, -6.5) and (33.0, -3.5, -6.2) in neutral state and oxidized state respectively. The Movie S1-S3 (supplementary information) show the reversible switching colours of polymer based devices between neutral and oxidized states.

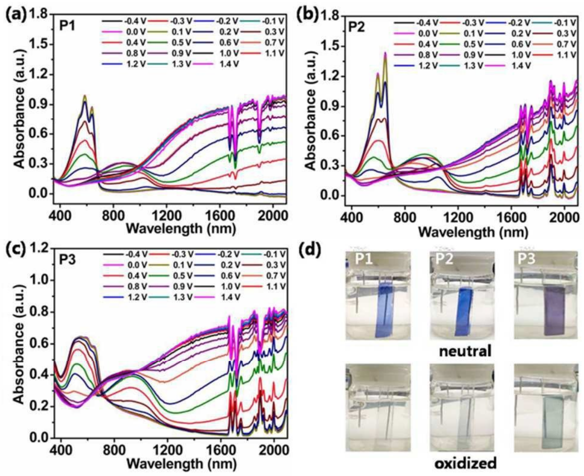

Fig. 2 (a) (b) (c) Spectroelectrochemistry of **P1**, **P2**, and **P3** films coated on ITO glass slides in a monomer-free 0.1 M TBAPF$_6$/ACN electrolyte–solvent couple at applied potential (-0.4 to 1.4 V) (d) Colors of the devices in their neutral and oxidized states.

Kinetic studies

For optical and electrochromic devices application, fast switching time of polymer thin films is favorable. Generally, films exhibiting high electroactivity or rough and porous morphology are highly beneficial for ions penetration, which results in a fast switching speed. Fig. 3 describes the optical transmittance of films as a function of time by applying square-wave potential method under external applied potentials of -0.4 V and 1.4 V in 0.1 M TBAPF$_6$/ACN system with a residence time of 10 s. The switching time of devices is calculated at 90% of full switching state. All the three devices present good stability and reversibility after several switching cycles at about 600 nm. Under applied potentials, the optical contrast measured between neutral deep blue and oxidized transparent colorless states is found to be 71% at 590 nm for **P1** film with a fast switching time of 1.10 and 1.80 s for coloring and bleaching respectively, which makes **P1** an attractive candidate for electrochromic applications. **P2** exhibits 61% of the transmittance changes at 650 nm with a complete coloring and bleaching in 2.0 s and 2.7 s while **P3** shows 35% of the transmittance changes at 600 nm with the switching time of 0.96 s for complete coloring and 1.63 s for bleaching. Noteworthily, all the three polymer films show higher optical contrast (about 60%) in near-IR region (about 1500 nm), which endow them potential application in NIR electrochromic devices, such as in buildings for environmental control of heat gain or loss.[16, 30] The difference of substituents in 3,6-position of thieno[3,2-*b*]thiophene core results in difference in interchain separation degree related to optical contrast and the upsurge in optical contrast of **P1** maybe because of the smaller bulk substituent[11].

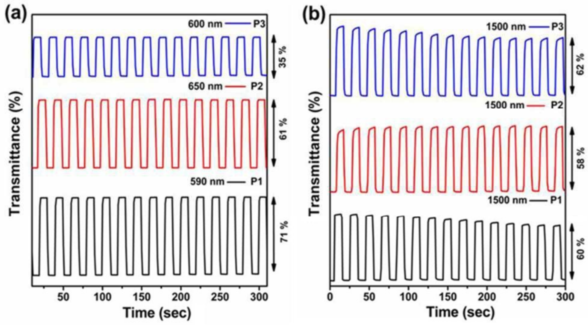

Fig. 3 Electrochromic switching percent transmittance change of polymer films coated on ITO glass slides monitored at (a) 590 nm for **P1**, 650 nm for **P2** and 600 nm for **P3** (b) 1500 nm for **P1**, **P2** and **P3** under exteral applied potentials of -0.4 V and 1.4 V.

To investigate the relationship between scan rates and current density, measurements were performed on the polymer thin films coated on Pt button electrode in 0.l M TBAPF$_6$/ACN system between -0.8 V and 1.4 V at the sacn rates of 25, 50, 75, 100, 125, 150 and 200 mV s^{-1}. The oxidation and reduction peaks show a corresponding increase in magnitude with the increase in scan rate as seen from Fig. 4(a), (b) and (c). Fig. 4(d) shows the linear dependence of the anodic and cathodic peak current densities on the scan rates, divulging the fact that the polymer films are electro-active, well adhered and the

View Article Online
DOI: 10.1039/C6PY00989A

electrochemical processes are reversible and not diffusion controlled.[31]

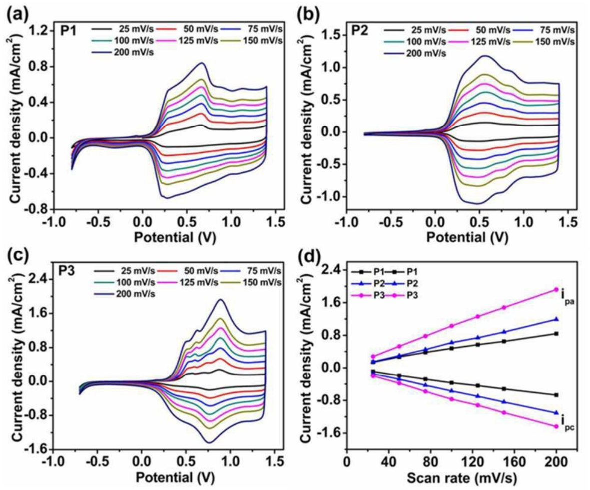

Fig. 4 (a) (b) (c) Scan rate dependence of P1, P2 and P3 films coated on Pt button electrode in 0.1 M $TBAPF_6$/CAN system at the scan rates of 25, 50, 75, 100, 125, 150 and 200 mV s^{-1} (d) a linear dependence as a function of the scan rate.

Morphology

Generally, the increasing film roughness and porosity facilitate the ions insertion and extraction to the film and make the redox process of the films easier. In order to probe the surface morphology of the polymer thin films, AFM was performed on electrochemically deposited polymer ITO films. As shown in Fig. 5, **P1** shows a quite homogeneous and flat morphology and has 10.5 nm roughness while both **P2** and **P3** have aggregation morphology. **P2** has a small granular structure while **P3** has a more elongated and well-aligned rod-shaped structure, which may facilitate the charge hopping mechanism.[32] The higher R_{RMS} of **P2** film (roughness of 31.1 nm) and **P3** film (roughness of 61.7 nm) is favorable to the doping/dedoping process, which leads to the better film stability and optical response than **P1**.

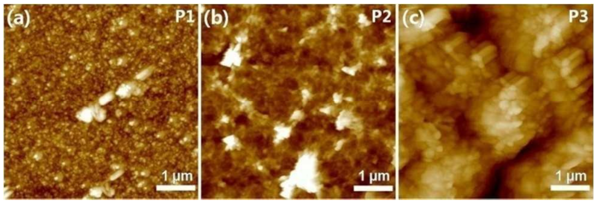

Fig. 5 (a) (b) (c) AFM images of polymer-coated ITO films. Scan size: 5×5 μm

SEM images (Fig. S1, supplementary information) of **P1** film exhibit a compact and homogeneous lamellar morphology, which is beneficial to increase the electrical conductivity and electron transfer capability of conjugated polymers, in addition, this morphology of the polymer films is also favorable in electrochromic devices fabrication[33]. Due to the intermolecular interaction resulted from alkyl chains, both **P2** and **P3** show crosslinked porous network morphology, which improves the redox stability because the counter-ions can move easily into and out of the polymer films during redox process.[16]

Stability

The stability of ECDs plays an imperative role in applications.[28] The polymer films coated on Pt button electrode were cycled 100 times in 0.1 M $TBAPF_6$/ACN system between their redox states with a scan rate of 100 mV s^{-1} in an open solution system. As shown in Fig. S2 (supplementary information), although the three polymers show a degradation trend after 100 cycles, interestingly, when the alkyl chains are introduced into the core, the resulting polymers show an increased stability of about 27%, which can be attributed to the ease of redox process brought by the increased surface roughness. The three polymers retained (67% for **P1**, 85% for **P2** and 84% for **P3**) reactivity after 100 cycles. For **P3**, a new peak appeared at 0.45 V which maybe because of the oxidation of a chain degraded from polymer.

Conclusions

The influence of different types of substituents on electrochromic behaviors has been studied. The different substituents on the 3,6-position of thieno[3,2-*b*]thiophene core initiate differences in electrochemical, optical and morphological behaviors. **P3** shows a blue shifted absorption in visible region compared with **P1** and **P2**. Consequently, the polymers **P1**, **P2** show deep blue while **P3** shows violet in neutral state. **P1** demonstrates the highest optical contrast up to 71% with a switching time of 1.10 s and 1.80 s for complete coloring and bleaching, but it shows a diminished stability. By the introduction of alkyl chains into the core, the surface roughness of resulting polymers increases, which results in an enhanced stability (from 67% improved to 85%, an increase of about 27%) after 100 cycles. The higher optical contrast of the three polymer films in near-IR region endow them potential application in NIR electrochromic devices. From these results, we conclude that substitution can be a subtle tuning method in electrochromic behaviors.

Acknowledgements

This work was financially supported by Shenzhen Key Laboratory of Organic Optoelectromagnetic Functional Materials of Shenzhen Science and Technology Plan (ZDSYS20140509094114164), the Shenzhen Peacock Program (KQTD2014062714543296, Shenzhen Science and Technology Research Grant (JCYJ20160331095335232 and JCYJ20140509093817690), Nanshan Innovation Agency Grant (No. KC2015ZDYF0016A), Guangdong Key Research Project

View Article Online
DOI: 10.1039/C6PY00989A

(Nos. 2014B090914003, 2015B090914002), Guangdong Talents Project , National Basic Research Program of China (973 Program, No. 2015CB856505), NSFC (51373075), and Guangdong Academician Workstation (2013B090400016).

Notes and references

1. J. R. Platt, *J. Chem. Phys.*, 1961, **34**, 862-863.
2. A. Michaelis, H. Berneth, D. Haarer, S. Kostromine, R. Neigl and R. Schmidt, *Adv. Mater.*, 2001, **13**, 1825-1828.
3. J. Remmele, D. E. Shen, T. Mustonen and N. Fruehauf, *ACS Appl. Mater. Interfaces*, 2015, **7**, 12001-12008.
4. R. J. Mortimer, *Chem. Soc. Rev*., 1997, **26**, 147-156.
5. B. Hu, C. Wang, J. Zhang, K. Qian, P. S. Lee and Q. Zhang, *RSC Adv.*, 2015, **5**, 77122-77129.
6. P. M. Beaujuge, S. Ellinger and J. R. Reynolds, *Adv. Mater.*, 2008, **20**, 2772-2776.
7. A. Durmus, G. E. Gunbas, P. Camurlu and L. Toppare, *Chem. Commun.*, 2007, DOI: 10.1039/B704936F, 3246-3248.
8. G. E. Gunbas, A. Durmus and L. Toppare, *Adv. Funct. Mater.*, 2008, **18**, 2026-2030.
9. C. M. Amb, J. A. Kerszulis, E. J. Thompson, A. L. Dyer and J. R. Reynolds, *Polym. Chem.*, 2011, **2**, 812-814.
10. J. Roncali, P. Blanchard and P. Frère, *J. Mater. Chem.*, 2005, **15**, 1589-1610.
11. B. Karabay, L. C. Pekel and A. Cihaner, *Macromolecules*, 2015, **48**, 1352-1357.
12. M. İ. Özkut, S. Atak, A. M. Önal and A. Cihaner, *J. Mater. Chem.*, 2011, **21**, 5268-5272.
13. J. F. Ponder, A. M. Österholm and J. R. Reynolds, *Macromolecules*, 2016, **49**, 2106-2111.
14. X. Chen, H. Liu, Z. Xu, S. Mi, J. Zheng and C. Xu, *ACS Appl. Mater. Interfaces*, 2015, **7**, 11387-11392.
15. B. Hu, M. Li, W. Chen, X. Wan, Y. Chen and Q. Zhang, *RSC Adv.*, 2015, **5**, 50137-50145.
16. H. Zhao, Y. Wei, J. Zhao and M. Wang, *Electrochim. Acta*, 2014, **146**, 231-241.
17. C. M. Amb, P. M. Beaujuge and J. R. Reynolds, *Adv. Mater.*, 2010, **22**, 724-728.
18. M. E. Cinar and T. Ozturk, *Chem. Rev.*, 2015, **115**, 3036-3140.
19. I. Meager, R. S. Ashraf, S. Rossbauer, H. Bronstein, J. E. Donaghey, J. Marshall, B. C. Schroeder, M. Heeney, T. D. Anthopoulos and I. McCulloch, *Macromolecules*, 2013, **46**, 5961-5967.
20. J.-I. Park, J. W. Chung, J.-Y. Kim, J. Lee, J. Y. Jung, B. Koo, B.-L. Lee, S. W. Lee, Y. W. Jin and S. Y. Lee, *J. Am. Chem. Soc.*, 2015, **137**, 12175-12178.
21. A. Balan, G. Gunbas, A. Durmus and L. Toppare, *Chem. Mater.*, 2008, **20**, 7510-7513.
22. G. Sönmez, I. Schwendeman, P. Schottland, K. Zong and J. R. Reynolds, *Macromolecules*, 2003, **36**, 639-647.
23. G. Sonmez, H. Meng, Q. Zhang and F. Wudl, *Adv. Funct. Mater.*, 2003, **13**, 726-731.
24. H.-M. Wang and S.-H. Hsiao, *J. Polym. Sci., Part A: Polym. Chem.*, 2011, **49**, 337-351.
25. P. M. Beaujuge, S. V. Vasilyeva, D. Y. Liu, S. Ellinger, T. D. McCarley and J. R. Reynolds, *Chem. Mater.*, 2012, **24**, 255-268.
26. H. Yu, S. Shao, L. Yan, H. Meng, Y. He, C. Yao, P. Xu, X. Zhang, W. Hu and W. Huang, *J. Mater. Chem. C*, 2016, **4**, 2269-2273.
27. T.-Y. Wu and Y. Chen, *J. Polym. Sci., Part A: Polym. Chem.*, 2002, **40**, 4452-4462.
28. P. M. Beaujuge and J. R. Reynolds, *Chem. Rev.*, 2010, **110**, 268-320.
29. Z. Shi, W. T. Neo, T. T. Lin, H. Zhou and J. Xu, *RSC Adv.*, 2015, **5**, 96328-96335.
30. G.-S. Liou, H.-J. Yen and M.-C. Chiang, *J. Polym. Sci., Part A: Polym. Chem.*, 2009, **47**, 5378-5385.
31. A. A. Kocaeren, *Org. Electro.*, 2015, **24**, 219-226.
32. J. Z. Low, W. T. Neo, Q. Ye, W. J. Ong, I. H. K. Wong, T. T. Lin and J. Xu, *J. Polym. Sci., Part A: Polym. Chem.*, 2015, **53**, 1287-1295.
33. K. Lin, Y. Zhao, S. Ming, H. Liu, S. Zhen, J. Xu and B. Lu, *J. Polym. Sci., Part A: Polym. Chem.*, 2016, **54**, 1468-1478.

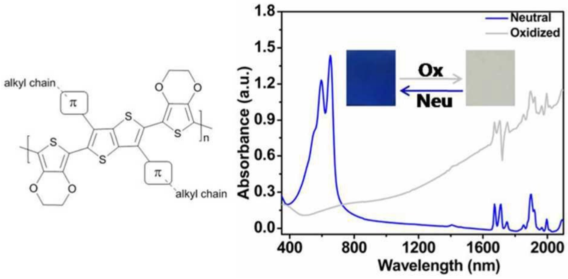

Polymers based on thieno[3,2-*b*]thiophene core modulated by alkylphenyl show high optical contrast and deep blue to highly transmissive electrochromic performances.